Root foraging alters global patterns of ecosystem legacy from climate perturbations

M. Berkelhammer, University of Illinois at Chicago (berkelha@uic.edu)
B. Drewniak, Argonne National Lab (bbye@anl.gov)
B. Ahlswede, University of Illinois at Chicago (bswede@uic.edu)
M.A. Gonzalez-Meler, University of Illinois at Chicago (mmeler@uic.edu)

Root foraging alters global patterns of ecosystem legacy from climate perturbations

M. Berkelhammer, [a] B. Drewniak,[b] B. Ahlswede,[a] M.A. Gonzalez-Meler,[a]

[a] *University of Illinois at Chicago, Chicago, IL, USA*

[b] *Department of Energy, Argonne National Lab, Lemont, IL, USA*

Corresponding author: Max Berkelhammer, berkelha@uic.edu

ABSTRACT: The response of terrestrial ecosystems to climate perturbations typically persist longer than the timescale of the forcing, a phenomenon that is broadly referred to as *ecosystem legacy*. Understanding the strength of legacy is critical for predicting ecosystem sensitivity to climate extremes and the extent to which persistent changes in land surface-atmosphere exchange might feedback onto the climate, for example, extending drought. The cause of ecosystem legacy has been tied to numerous factors such as changes in leaf area index, however, few studies have tested how changes in root profiles in response to stress might alter an ecosystem's recovery time. We utilize an Earth System Model that includes a dynamic root module where vegetation can forage for water and nutrients by altering their root profiles. As expected, the simulations show that in response to water stress events most ecosystems deepen their root profiles. In semi-arid ecosystems, this response expedites recovery (i.e. less legacy) relative to simulations without dynamics roots because access to deeper water pools after the initial event remains favorable. In wetter ecosystems, the development of deeper root profiles slows down the recovery timescale (i.e. more legacy) because the deeper root profile reduces access to nutrients. The recovery of hyperarid systems is also delayed presumably to the loss of shallow roots and ability to access water from smaller rain events. The results show that the response of root profiles to external forcing is a critical component of global patterns of legacy that is not typically represented in Earth System Models.

1. Introduction

Ecosystems across all global biomes display some varying level of sensitivity to antecedent conditions. Key ecosystem processes such as transpiration, CO_2 flux and shortwave absorption are thus not only instantaneously responding to external conditions but display a response that integrates the conditions over recent hours, days or years (Ogle et al. 2015). This is a coupled climate-ecosystem phenomenon referred to as "legacy" or "memory" that emerges from internal ecosystem dynamics and is distinct from the persistence of climate or weather patterns that might arise from lower frequency ocean-atmosphere modes such as ENSO (Kumar et al. 2019; Bunde et al. 2013). While legacy effects have been observed and classified by ecologists for decades, it is a topic that has received renewed interest recently owing both to concerns that the effects of more frequent extreme events could be compounded by persistent legacy leading to mortality or bifurcation (McDowell et al. 2013; Anderegg et al. 2013; Trugman et al. 2018; Szejner et al. 2020) and the recognition that the predictive skill of models is limited without considering these effects (Anderegg et al. 2015; Kolus et al. 2019). With respect to the latter, the lack of realistic legacy effects in land surface models is problematic because Earth System Models (ESMs) exclude feedbacks that might act to amplify or extend climate extremes (Miralles et al. 2019; Fischer et al. 2007). For example, an extended reduction in transpiration for months or years after a drought would lead to an increased contribution of sensible (relative to latent) heat fluxes from the surface (Yunusa et al. 2015; Donat et al. 2018). Improved knowledge of the mechanisms driving legacy and their integration into land surface models is thus an important trajectory for Earth System Model development.

From the standpoint of climate feedbacks, ecosystem legacy effects can involve a variety of processes such as direct changes in carbon (Gross Primary Production-GPP- or respiration), water (transpiration) or energy fluxes or shifts in aboveground biomass that affect frictional and radiative properties of the land surface (Galiano et al. 2011; van der Molen et al. 2011; Dewar et al. 1994; Liu et al. 2019). The various observational tools that have been utilized to quantify ecosystem legacy such as tree ring records (Gazol et al. 2020; Kannenberg et al. 2019; Peltier and Ogle 2020), eddy covariance (Liu et al. 2019) and satellite retrievals (Seddon et al. 2016; Kolus et al. 2019) have distinct sensitivities to these different legacy components (Ogle et al.

2015). For example, tree ring records are a direct indicator of carbon allocated to woody biomass, eddy covariance provides information on land surface-atmosphere exchange whereas satellite retrievals of emissivity (e.g. MODIS) or canopy structure (e.g. LiDAR) are sensitive to canopy physical and radiative properties. While these approaches provide overlapping information (e.g. tree ring growth is partially controlled by carbon uptake (Campioli et al. 2016)), the different approaches also yield seemingly disparate information. For example, Kannenberg et al. (2019) and Gazol et al. (2020) both note that sustained reductions in tree ring widths following drought were not mirrored by persistent reductions in satellite indices of greenness or plot-scale GPP. These differences could reflect distinct components of legacy or biases in the observational tools. For example, satellite retrievals may lack sufficient sensitivity to capture subtle legacy effects or simply miss changes in below-canopy dynamics. Reconciling this information to develop a clearer picture of the timescales and strength of legacy within different components of ecosystems is key for diagnosing missing legacy dynamics in land surface models.

By taking advantage of the different observational and statistical approaches as well as efforts to experimentally perturb ecosystems (Gonzalez-Valencia et al. 2014; Herzog et al. 2014; Belk et al. 2007; Zweifel et al. 2020; Liu et al. 2019; Ogle et al. 2015; Jiang et al. 2019), a clearer picture has begun to emerge about mechanisms driving legacy (Monger et al. 2015; Kannenberg et al. 2020; Ovenden et al. 2021). These mechanisms include changes in allocation between and within above- (leaf, wood, stem) and belowground (roots) carbon pools (Phillips et al. 2016; Zweifel et al. 2020), damage to organs such as embolisms in xylem tissue or reduced stomatal control (McDowell et al. 2013), exhaustion or buildup of stored carbon pools (Richardson et al. 2015), changes in the water table depth or deep soil moisture (Sala et al. 1992; Amenu et al. 2005; Kumar et al. 2019) and shifts in vulnerability to pests or pathogens that can extend the effects of an isolated climate event (Flower and Gonzalez-Meler 2015). Shifting allocation patterns between leaves, woody biomass and fine roots has emerged as a critical and ubiquitous source of legacy. This effect can be predicted from ecological theory on optimizing resources (water, nutrients and light) to maximize profits (carbon pools) (Thornley 1998; McCarthy and Enquist 2007; Poorter et al. 2012; Bloom et al. 1985; McNickle et al. 2016). It follows that drought stress - the most widespread global cause of seasonal to interannual ecosystem stress (Seddon et al. 2016) - leads

to both reduced total carbon pools and increased investment of those pools below ground to forage for water (Drewniak 2019; Brunner et al. 2009; Markewitz et al. 2010; Metcalfe et al. 2008; Joslin et al. 2000; Lu et al. 2019). The loss of carbon dedicated to leafy material in exchange for root mass leads to a persistent multi-year legacy on primary productivity and consequently resources available to rebuild the canopy (Galiano et al. 2011; Zweifel et al. 2020). On the other hand, drought stress may not change carbon allocated to leaves and instead shift allocation only between wood and fine roots and thus have a minor impact on aboveground greenness but have an extended impact on belowground processes and nutrient and water access (Doughty et al. 2014; Dybzinski et al. 2011; Phillips et al. 2016).

We focus hereafter on this question of how dynamic changes in the depth distribution of fine roots following stress events influences the recovery of an ecosystem. Although some observational studies have supported theoretical predictions where stress promotes shifting carbon investment belowground (Markesteijn and Poorter 2009; Canadell et al. 1996; Schenk and Jackson 2002), this effect is not consistently borne out and does not necessarily predict how a change in investment in root systems influences ecosystem recovery or legacy. On the one hand, the investment in deeper roots following drought could expedite recovery if the modified root distribution proves beneficial. For example, an initial dry period may lead to a persistent reduction in root zone moisture or a drop in the water table (Kumar et al. 2019; van der Molen et al. 2011; Monger et al. 2015). In this case, the investment in a deeper fine root pool would expedite recovery and reduce legacy by "anticipating" sustained water stress. On the other hand, the initial response to forage for water with deeper roots may slow down the recovery if the root profile is now "maladjusted" (Zweifel et al. 2020) and the reduced access to shallow water and nutrients delays recovery. In this case, legacy of a drought could be extended by the change in root structure.

In ecosystems with long-lived species, the root response to drought may over time lead to root systems that are catered to reduce vulnerability to extreme water stress events. This can generate a circumstance where during optimal climate states, when water is not limited, the root systems are suboptimal due to their life history. It is thus also instructive to explore the legacy associated with optimal or unstressed growth periods i.e. pluvial states. In this case, root systems would shallow

enabling greater access to nutrients and near surface soil moisture, that has less hydraulic cost, when water availability is plentiful. The shallower root system could either allow the ecosystem to remain highly productive and extend the legacy of the bountiful times or leave the system vulnerable to future periods of water limitation especially if moisture limitation is the typical state of the system (Jiang et al. 2019). Having a dynamic root structure could thus have the effect of either increasing or decreasing the strength of legacy but how these responses manifest across global bioclimate gradients has not yet been tested (Phillips et al. 2016).

The response of root systems to an exogenous forcing like drought is itself complicated to predict (Metcalfe et al. 2008; Hendrick and Pregitzer 1996) and whether this change enhances or diminishes legacy is largely unknown (Brunner et al. 2009; Phillips et al. 2016). Observational studies show that the response of roots to climate forcing and the cascading effects these changes have on productivity are a function of soil structure and nutrient availability, plant type, severity and length of the climate anomaly and background climate state making it difficult to scale up from local studies (Matamala et al. 2003; Doughty et al. 2014; Germon et al. 2020; Warren et al. 2015; McCormack et al. 2015; Kou et al. 2018). One way to develop more universal hypotheses on the role of roots in generating ecosystem legacy is to explore how legacy in land surface models is affected by changing root profiles. Land Surface Models that include dynamic roots have been developed (Lu et al. 2019; Drewniak 2019; El Masri et al. 2015; Bouda and Saiers 2017; Sakschewski et al. 2021) and these can be implemented into ESMs and forced with a broad spectrum of climate inputs across global biomes. For example, Drewniak (2019) recently implemented a dynamic root module into the Energy Exascale Earth System Model (E3SM) and reproduced some of the key features observed in root profile measurements including a consistent deepening of roots in response to water stress. While the model somewhat failed to capture root profiles in some ecosystems, such as the dimorphic pattern of roots in the dry tropics (Sakschewski et al. 2021), the addition of dynamic roots did modestly improve global estimates of productivity. Similarly, Lu et al. (2019) developed a 3-dimensional dynamic root module that allowed root systems to develop from a null state. They also reproduced similar dynamic deepening of roots in response to reduced water availability and simulated the evolution of root profiles as stands age consistent with data from chronosequences. Using

a production function and a game theoretical approach, McNickle et al. (2016) was able to reproduce the above- and below-ground patterns of net primary productivity and ecosystem fluxes consistent with FluxNet and MODIS data. While these models are limited in their ability to simulate root morphology, root phenology, dynamic allocation, response to stress and soil moisture-groundwater interactions they, nonetheless, provide a framework to consider questions of how foraging patterns in roots alter ecosystem legacy strength and timescale across biomes.

In this paper, we utilize a pair of global ESM simulations forced with historical climate in both a default model (fixed root profiles) and with the inclusion of a dynamic root profile module (Drewniak 2019). In Section 1 of the study, we assess how well the control simulations reproduce the legacy of GPP with respect to satellite observations. In Section 2, we classify how root systems respond to positive and negative events using a clustering algorithm to identify dominant global patterns in root response to perturbation across biomes and plant functional types. In Section 3, we assess the extent to which the different responses of root profile to perturbation either enhanced legacy or whether the root profile adjustment to perturbation led to more optimal states that expedited recovery. The results presented clearly illustrate that legacy is globally affected by root dynamics and we conclude the paper by discussing the implications this finding has for improving the ability of ESMs to capture realistic ecosystem legacy characteristics.

2. Methods

a. Model simulations

All E3SM simulations were performed in offline mode with a post v1 version of the E3SM Land Model (ELM) (Golaz et al. 2019) using atmospheric forcing from the Global Soil Wetness Project 3 (GSWP3; (Dirmeyer et al. 2002)) at a resolution of 0.5° by 0.5°. Model spinup was performed by cycling the GSWP3 over the years 1901-1920 until reaching steady state following the accelerated decomposition and regular spinup procedures recommended by Thornton and Rosenbloom (2005). Following spinup, both simulations used the same GSWP3 forcing over the historical period 1901-2010. We utilize outputs from 2 simulations referred to hereafter as *No Dyn.* and *Dyn.*. The *No Dyn.* simulation is the control run in the default ELM configuration

without dynamic roots. The *Dyn.* simulation was performed with dynamic roots turned on and with an increase in the weight given to water in the root foraging scheme by setting f to ≤ 0.5 as in Drewniak (2019). This does not affect the actual water stress in the vegetation but reduces the minimum preference for roots to seek soil layers with water to facilitate more foraging dynamics. Within the *Dyn.* simulation we also increased the root turnover time from 1 to 2 years to enhance root legacy but this had virtually no impact on the results compared with simulations run with turnover time kept at default.

From the historical E3SM simulations, we extract monthly-averaged GPP, transpiration, relative fine root fraction per soil layer, temperature and precipitation as well as the distribution of PFTs from each grid cell (Table 1). As noted above, studies on legacy have relied on a wide variety of metrics to quantify legacy ranging from tree ring growth, canopy structure or net ecosystem exchange of carbon (Kannenberg et al. 2020; Liu et al. 2019; Sala et al. 2012). We utilize model outputs of GPP and its persistence following perturbation as the ecosystem metric to track legacy because GPP is closely linked with the overall ecosystem carbon pool available to recover from (or extend) an event and also that satellite estimates of GPP from solar-induced fluorescence (SIF) and near infrared reflectance (Section 2.2) provide a global-scale and independent benchmark to compare simulated legacy effects against. After extracting the GPP data from the simulations, we apply a PFT filter to remove grid cells that do not have a dominant PFT - defined here as grid cells where a single PFT accounts for $\geq 50\%$ of the grid area. The reason for this filtering was to balance the need to use grid-averaged data to facilitate comparisons with the satellite data while also ensuring each grid cell can be associated with a specific PFT to facilitate analysis of PFT-specific dynamics. For each grid cell, we generated monthly GPP anomalies by detrending each month of the timeseries over the last 50 years of the simulations. This approach to generating anomalies produces a similar result as the more common approach of subtracting the mean seasonal climatology from each year but is used here because it also removes any low frequency trends in the data. Because some grid cells show sustained trends in GPP, failing to detrend can lead to artificially high estimates of short term legacy.

b. Satellite and meteorological data

To provide a benchmark to compare the modeled estimates of legacy against, we used the 0.5° by 0.5° satellite derived estimates of GPP from Joiner et al. (2018). This product provides monthly estimates of GPP from 2001-2020 using a combination of SIF and MODIS reflectance along with a light use efficiency model. The product was calibrated against data from a network of global Eddy Covariance sites but the estimates do not rely on a model that is forced with meteorological data which means we can treat the estimates of legacy from the satellite data as independent from those derived from the E3SM simulations. We reiterate that the goals here were not to use the satellite data to critique the ESM estimates of legacy but rather to ensure the simulations produced realistic estimates of legacy. We note that differences between model and satellite-estimated legacy may not be strictly from a bias in the model because the satellite estimates have their own limitations due both to a lack of sensitivity in some ecosystems and that the satellite timeseries is relatively short (20 years) with respect to properly characterizing typical responses to perturbations that are uncommon by definition.

In addition to the satellite GPP data, we also utilize a merged satellite and meteorological aridity index (AI) product - defined as the ratio of precipitation to potential evapotranspiration - to classify the average degree of water stress at each grid cell. The aridity index provides a holistic perspective on water stress because it accounts for both the effects of precipitation and evaporative demand on water availability (Arora 2002). For this study, we use the globally-derived estimates of AI from Trabucco and Zomer (2018) that combine weather data from meteorological stations (wind, precipitation, temperature and humidity) and radiation data from MODIS to estimate both precipitation and potential evaporation from the Penman-Monteith equation. Locations with an AI greater than 1 are not chronically water-limited while sites with values less than 1 have a theoretically higher water demand than is input from precipitation. Using AI, sites can be classified along a *super-arid* to *super-humid* gradient based on their unitless AI value.

c. Classification of legacy

There exists a wide range of approaches to classify legacy though they all depend fundamentally on defining how long it takes for the system to return to an unperturbed state (Ogle et al. 2015; Monger et al. 2015; Liu et al. 2019; Kannenberg et al. 2019). Definitions of legacy can be framed in terms of strength (i.e. how sensitive the system is to the previous state) or in terms of timescale (i.e. the length of time it takes for the system to return). For example, a system could display an initially rapid recovery but require an extended period to fully return to pre-disturbance state leading to a long legacy timescale but weak effect. For individual sites, definitions of legacy and the statistical choice can be more tailored to the local dynamics but for global analyses, generalized and transferable approaches are required (Kolus et al. 2019). We opted here for two relatively simple definitions of legacy that target the strength, rather than the timescale, and can be easily implemented across ecosystems. For the first definition of legacy, we integrate the partial autocorrelation function of de-seasonalized GPP anomalies across a 1-12 month lag. This is a unitless value that captures the strength of persistence in GPP anomalies. While it is a robust metric that is widely used in many timeseries applications, it has a few critical limitations that need to be addressed in the context of this study. Firstly, the autocorrelation function does not distinguish between endogenous (internal ecosystem processes) and exogenous (externally-forced) sources of legacy. For example, a region where precipitation anomalies persist across months would likely have a high degree of apparent GPP legacy that is not related to an ecosystem dynamic. In other words, some component of legacy defined using this approach is just the expected response of the ecosystem to an instantaneous forcing that happens to have intrinsic autocorrelation. This limitation is acceptable here because we compare simulations with and without dynamic roots that are both forced with the same climate. Therefore differences in the autocorrelation between the control and experimental simulations must arise not from the climate forcing but from the ecosystem processes that are altered by the presence of dynamic roots.

The second limitation of the autocorrelation approach is that it does not distinguish between the strength of legacy associated with positive vs. negative perturbations. We address this issue by utilizing a second approach to defining legacy based on identifying positive and negative GPP "events" in the timeseries' from each grid cell and estimating the recovery time associated with

these events. In contrast to some previous studies, we did not look for droughts or pluvial events defined by climate anomalies but instead classify GPP "events" or perturbations as those when GPP exceeded ±1 standard deviation from the mean detrended monthly state at that grid cell. This allows us to quantify legacy across ecosystems that may have distinct limiting factors for GPP. To do this, we normalized GPP anomalies using a z-score and identified each month when the normalized GPP anomaly exceeded ±1 while also meeting the conditions that an anomaly of this size had not occurred in the previous three months (to avoid double counting events). We then took the sum of the normalized GPP anomalies for the 12 months following the initial event. The sum provides an integrated value for the strength of the legacy while not, per se, identifying the length of time the recovery took. The end product are two additional definitions of legacy for each grid cell based on the direction and strength of GPP anomaly persistence following both positive and negative events.

d. Classifying the response of root profiles to perturbation

Monthly root profiles for each depth (n=15) were converted to anomalies by detrending each month and depth of the relative fine root fraction. As with the approach to generating GPP anomalies, the detrending of the root fraction removed any seasonal cycles or long term trends in the root fraction for each depth. Using the technique to identify GPP events (either positive or negative) as described in Section 2c, we capture the root profile anomalies for the 12 months following these events. We then average the root profile anomalies (with dimensions of 12 months by 15 depths) for all GPP events within each grid cell to generate an average root profile response to positive and negative GPP events. The end product is a matrix of root profile anomalies for positive and negative GPP events for every grid cell. To identify canonical patterns in how root profiles respond to positive and negative GPP events, we utilize a *k-medoid* clustering algorithm to minimize the global dataset into a finite number of dominant root response patterns. The goal of the clustering algorithm is to divide the root profile anomalies into a pre-defined number of clusters that minimizes the sum of distances between each root profile within a cluster while maximizing the difference between clusters. Unlike k-means clustering, where the centroid of a cluster is the average of all members of the cluster, the centroid of each cluster in the k-medoid

algorithm is a member of the cluster (i.e. a medoid). The clustering uses an iterative approach where first an initialization procedure identifies possible centroids and then organizes all the root profiles into the the most similar medoid, minimizing distance between each member of the cluster and the centroid. This procedure is then repeated with a new set of medoids to see if a better solution is reached, i.e. where distance between clusters is increased and distance between members of the same cluster is decreased. This iterative process repeats with a new selection of medoids until no further gains are achieved. To implement this algorithm, two things need to be assigned *a priori*: (1) the number of clusters and (2) the metric to estimate distance. We chose 4 clusters, which led to some redundancy among cluster shapes but also effectively captured key structures without having too many clusters with small populations of uncommon root responses. The distance metric was based on the Minkowski method (Kaufman and Rousseeuw 2009), though other methods such as *City Block* yielded similar results.

e. Quantifying the role of root dynamics in legacy

After identifying the dominant root profiles in response to perturbation (Section 2d), we then assess whether a particular root response increases ecosystem legacy through a comparison between legacy strength in simulations with or without dynamic roots which we refer to as Δ Legacy. For example, a particular root structure that was classified as *Cluster 1* might emerge in 1000 grid cells. The legacy strength in these 1000 grid cells forms a distribution that can be subtracted from the legacy strength of these same grid cells from the simulation that does not include dynamic roots (i.e. the Control). This process is repeated for each of the root profile clusters to assess whether particularly root responses to perturbation have the effect of adding or subtracting ecosystem legacy. We conclude the analysis by assessing whether the strongest increases or decreases in legacy associated with a particular root response can be tied to specific PFTs or climate.

3. Results

Our analysis of legacy from satellite GPP retrievals reveals a broad range of legacy strength that varies significantly by region and PFT (Fig. 1). The highest levels of legacy emerge in the broadleaf deciduous temperate shrubs (BDTS) that dominate Australia, southern South America

and regions of northern Mexico and the southwestern US. Following this, the broadleaf deciduous and evergreen forests prevalent in the Amazon and the maritime continent (BDTrT and BETrT) dominate the other continuous areas with high legacy. While other regions such as Alaska, coastal regions of the western US, SE Asia, western India and the Iberian Peninsula also show regionally high legacy, the majority of PFTs show similar median values and ranges in terms of legacy strength. Part of the spatial pattern in legacy strength likely reflects the length of the growing season where regions with longer growing seasons are more prone to persistent GPP anomalies for months whereas the boreal systems are productive for too short a period of the year to demonstrate significant intra-annual legacy. However, the range of legacy within almost all the PFTs is large, indicating the value cannot simply be explained as a function of PFT or latitude.

The spatial pattern in legacy that emerges based on the autocorrelation definition (Fig. 1a-b), shares similarities to the legacy defined through the response of GPP anomalies to positive and negative events (Figs. 1c-f). For example, Australia, the maritime continent, southern South America, southern Africa, the Iberian Peninsula and western North America (Alaska to Mexico) all show consistently strong legacy strength across all metrics. Similarly, boreal systems and C3 agroecosystems (silviculture and herbaceous) are all characterized by low legacy across the definitions. Some notable differences include the unremarkable legacy associated with positive and negative events in the Amazon. Because our focus is on the effects of dynamic roots on legacy, we restrict interpretation of the global characteristics of legacy to future studies and simply use the data from Figure 1 as a benchmark to compare the simulated data against.

The control simulations without dynamic roots broadly reproduced the global patterns of legacy derived from satellite and capture how the strength of autocorrelation varies between the PFTs (Figs. 2b and d). The simulations do, however, typically overestimate autocorrelation as indicated by the fact that the range data for most PFTs fall above the 1:1 line relative to satellite data. This high bias is clearly apparent in tropical Africa, parts of the Amazon and across the southern US (Figs. 2a and c). In contrast, the simulations underestimate autocorrelation in Australia and the maritime continent. From the standpoint of providing a benchmark, the comparison with the satellite data indicates that the control simulation generates broadly realistic

results across PFTs. Another critical benchmark for the control simulations is whether it produces realistic recovery rates from positive and negative GPP events. We consider this by comparing the covariation between negative and positive legacy strength for the different PFTs (Fig. 3). The satellite data show a strong correlation between the legacy strength associated with positive and negative events but indicate that legacy from positive events is modestly stronger than that for negative events (Fig. 3a). In other words, positive GPP anomalies are more persistent than negative ones. This effect is less well produced by the control simulations, which show less legacy associated with both positive and negative events and that the magnitude of positive and negative legacy are similar. However, despite these issues, the range of negative and positive legacies in the simulations falls within the range defined by the satellite benchmark.

As noted, one of the limitations to the statistical approach to define legacy here is that it does not isolate endogenous or biotic sources of persistence (e.g. pests or competition) from exogenous sources (i.e. climate or weather). While this issue does not affect our conclusions on how dynamic roots influence legacy, it is still valuable to highlight whether and how exogenous forcing influences global patterns in GPP legacy. To assess this, we compared the legacy in GPP with temperature and precipitation autocorrelation from the same grid cells (Fig. 4). The persistence in temperature and precipitation anomalies were de-trended and de-seasonalized and defined using the same unitless metrics as GPP (Section 2c) and therefore can be compared directly against GPP legacy. The results from this analysis show how the majority of PFTs fall along a line that defines an expected response of GPP to intra-annual persistence in weather conditions (Figs. 4a and c). However, we also note that this linear relationship starts to fail for some of the PFTs that displayed the highest legacy including the broadleaf evergreen tropical and temperate forests and the tropical deciduous ecosystems. The former displays less legacy than expected (i.e. a weaker coupling to weather) whereas the latter shows higher GPP legacy than expected from temperature and precipitation autocorrelation. The same tight coupling of GPP to temperature and precipitation legacy is also present in the control simulations (Figs. 4b and d). However, relative to the satellite data (Figs. 4a and c), the simulations show an even tighter coupling to temperature and precipitation. For example, whereas satellite data from the broadleaf evergreen ecosystems seem to deviate from the other PFTs, data from this PFT in

the simulations falls more clearly along a continuum with the other ecosystems. Similarly, the broadleaf deciduous forests, do not display the distinct behavior seen in the satellite retrievals. In presenting the model vs. satellite comparison, it is important to note that the simulations are directly forced by the weather data (i.e. the weather data is "perfect") whereas the satellite data is forced by actual conditions that can never be perfectly captured by gridded weather products.

We focus hereafter on how legacy varies between simulations that include and exclude dynamic roots to illustrate the way root foraging modulates legacy. The presence of dynamic roots leads to an increase in legacy across the Amazon, Congo, southern Africa, northern Australia while root foraging decreases legacy in savannahs to the north and south of the Congo basin, the dry subtropical boreal forests of South America, the midwestern US, northern Europe, SE Asia and the temperate broadleaf forests in northern Europe (Fig. 5a and b). However, most of the PFTs show no systematic change in legacy with the addition of dynamic roots but do show a large range of responses between grid cells that share the same PFT. In other words, dynamic roots did not systematically alter global patterns of legacy in one direction but the wide range of values within each PFT show that the local impact of dynamic roots on legacy strength are significant. In addition to classifying the changes of legacy by PFT, we also assessed how water stress, defined using AI, modulated the role of dynamic roots in affecting legacy (Fig. 5b and d). This analysis shows how both wet (humid to super humid) and the most chronically water-stressed (super arid) sites displayed an increase in legacy with dynamic roots. In contrast, the semi-arid sites showed a general loss of legacy.

To understand how the presence of dynamics roots influences legacy, we assessed whether specific changes in the root profile (e.g. deepening or shallowing) enhanced legacy strength. In other words, if a negative perturbation in GPP was associated with investment in more shallow roots at one site and deeper roots at another site, we would not necessarily expect that legacy in these two sites would be affected in the same direction. As discussed in Section 2d, we used a clustering algorithm to blindly classify root structural responses, allowing us to organize grid cells with similar root responses to perturbation. As an example result, Figure 6 shows the average root response to perturbation for all grid cells from one of the clusters.

As expected, following a declining GPP event, there was a relative loss of fine roots above 10 cm and an increase between 10 to 100 cm, with the change centered around 20 cm (Fig. 6a). The redistribution of roots relaxes over time and the system returns to its mean root profile state after ~10 months. An almost perfectly complementary pattern emerges following positive GPP events, where a relative accumulation of roots above 10 cm was supported by a relative loss of roots from 10 to 150 cm, centered around 80 cm (Fig. 6b). As with the negative GPP response, this pattern decays and the root profile returns to its mean state by ~10 months.

The root distribution patterns shown in Figure 6 provide an example of one of the four defined root responses to perturbation. As expected, this pattern was the most widespread global response to a negative GPP event, i.e. where ecosystems gain deep roots at the expense of shallow roots (Fig. 7a and b). Variants of this pattern are captured by two separate clusters with one being extremely widespread and associated with modest changes in root distributions ("Cluster 1", Fig. 7a) and the second variation being associated with a response that was less prevalent but with a significantly larger redistribution of roots ("Cluster 2", Fig. 7b). The canonical pattern that was captured by the two clusters spans sites across the globe and examples of this root response to perturbation emerged at least periodically in every PFT (Figs. 7a and b). Complementary versions of the two variations of this pattern emerge in response to positive GPP events where shallow roots increase at the expense of deeper roots (Figs. 8a and b). As with the response to negative GPP events, the pattern of shallower roots was decomposed into two variants with one being extremely widespread but only a modest change ("Cluster 1", Fig. 8a) and the other being less widespread but a more dramatic redistribution of roots ("Cluster 1", Fig. 8b). The prevalence of these particular patterns reflects that the GPP events were mostly driven by changes in water availability that drove water foraging to deeper horizons following negative GPP events and foraging for shallow water and nutrients during periods of water abundance (Drewniak 2019; Lu et al. 2019).

Although there was a clear global dominance of the root patterns captured by Clusters 1 and 2, there were also root profile changes in response to perturbation that were significantly different in structure. For example, the grid cells that fell into Clusters 3 and 4 capture populations of sites where the ecosystems surprisingly lose deeper roots (60-100 cm) following negative GPP events and gain deeper roots following positive GPP events (Figs 7c-d and 8c-d). The grid cells

associated with Cluster 3 display a dimorphic pattern, where the loss of deep roots following negative events was also associated with marginal root loss near the surface. The number of grid cells displaying this behavior was significantly smaller and were generally found in Arctic and alpine sites though scattered examples of this response can be seen elsewhere including in parts of the Sahel, Australia and SW US.

Despite the fact that the population of sites within each cluster are defined by their similar root response to perturbation, the change in legacy (i.e. Δ Legacy) associated with sites from each cluster did not generally produce a uniform change in legacy direction (Fig. 9). For example, the 1000's of grid cells that fall into cluster 1, produced a wide response in legacy relative to the control. This is to say that, on average, the deepening of roots associated with water stress does not systematically increase nor decrease legacy. To gain insight into why the same root response could generate either an increase or decrease in legacy, we isolate the grid cells from within the population that display either the largest increases (90^{th} percentile) or largest decreases (10^{th} percentile) in legacy relative to the control simulations and assess the conditions that define these grid cells (Fig. 9). This analysis shows that the mean level of water stress at a site modulates whether foraging for water acts to increase or decrease ecosystem legacy. In the case of Cluster 1, the deeper roots following negative GPP events, had the effect of adding legacy for the non water-limited sites (i.e. AI$\geq$1) but decreased legacy at the semi-arid sites (i.e. AI$\geq$0.3 and AI$\leq$1). For Cluster 2, we also see that the deeper roots following stress events leads to a decrease in legacy at the semi-arid sites but, surprisingly, an increase in legacy at the super-arid sites.

Although the canonical pattern of deepening roots following stress events does not produce a singular type of effect on legacy, the more complex dimorphic pattern associated with Cluster 3, produces a nearly universal increase in legacy for all sites that displayed this dynamic (Fig. 9). In other words, in locations where both deep and shallow roots are lost in exchange for investment in roots at intermediate depths, negative GPP anomalies were persistently extended. This occurred even though this root pattern tended to only emerge at semi-arid sites which otherwise generally displayed a loss of legacy strength when dynamic roots were enabled in the model. Although the root pattern defined by Cluster 3 shares some similarity to the pattern defined by Cluster 4, the

sites associated with the latter did not generate a uniform increase nor decrease in legacy. These sites that developed a shallower root profile in response to negative events follow a pattern where drier sites (all sites with AI≤1) show a decrease in legacy whereas the wetter sites show added legacy - similar to the effect of water stress on legacy as seen in sites that fell into the Cluster 1 pattern.

Although the analysis thus far has largely focused on legacy of GPP in response to perturbation, we also compare the legacy response of transpiration to dynamic roots. Legacy in transpiration is key to predicting the recovery timescale for energy partitioning (latent vs. sensible heat) and surface boundary layer coupling. On the one hand, we assume that because transpiration and GPP are strongly coupled legacy of GPP would be mirrored by changes in the legacy of transpiration. However, we did not know whether different root responses to GPP events (Figs. 7 and 8), might modulate the relative time scales at which GPP and transpiration recover. Our comparison between the effect of dynamic roots on GPP and transpiration legacy shows there is an extremely strong similarity between the two (Fig. 10). The nearly identical 1:1 response between GPP and transpiration legacy is manifest across all of the different patterns in the root response to perturbation (i.e. Clysters 1-4), indicating that all the discussion thus far on the role of roots in affecting GPP legacy can be applied when discussing transpiration legacy. Sites where dynamic roots extend GPP recovery times are also sites that show proportionately similar changes in transpiration recovery. The one exception emerged within the Broadleaf Evergreen Tropical forests (Figs. 10a and e) (Sakschewski et al. 2021). At these sites, changes in transpiration and GPP legacy are largely decoupled and the effect of roots on GPP legacy proved modest relative to the effect of root foraging on transpiration legacy.

4. Discussion

Existing studies that have focused on ecosystem legacy have found that ESMs tend to underestimate the strength and timescale that ecosystems are affected by antecedent conditions (Kolus et al. 2019). This has been attributed to missing factors that carry previous conditions forward. Building from this work, we used a pair of general metrics to define legacy in GPP from both

simulations and satellite data (Figs. 1 and 2). We applied this analysis across all terrestrial biomes and found that the E3SM model - a state-of-the-art ESM - generally underestimated the legacy associated with both negative and positive GPP events (Fig. 3). Furthermore, the simulations did not reproduce the slightly asymmetric behavior seen in the satellite data where legacy associated with positive events was stronger than from negative events (Jiang et al. 2019). This finding is somewhat novel as previous studies have tended to focus more on recovery from drought (Gonzalez-Valencia et al. 2014; Anderegg et al. 2015; Kannenberg et al. 2020) but is not surprising in that the complex ecosystem dynamics that drive legacy would optimally respond to shorten effects from stress and extend effects of positive conditions. In addition, the simulations tended to overestimate autocorrelation in GPP anomalies which we attribute to the fact that modeled estimates of productivity tend to be too tightly coupled to weather forcing which, naturally exhibits a relatively high level of persistence in most regions (Fig. 4). These results largely met our *a priori* expectations and highlighted, as noted above, the presence of missing endogenous factors in ESMs that carry ecosystem memory forward.

Of the potential drivers that might explain the missing sources of legacy, we have focused here on the specific role that changes in root profiles have on GPP and transpiration memory following perturbation. In reality, the potential role of roots on legacy is far more complex than simply a dynamic depth profile and includes changes in root morphology, hydraulic redistribution, root turnover, soil biogeochemical cycles and microbial structure. However, we use this particular aspect of root dynamics to illustrate the potentially critical and under-represented role for roots in developing more realistic legacy structure in ESMs. We intentionally amplified these effects both by increasing apparent water stress factors to drive more water foraging in the roots and extending the turnover time of fine roots so that changes in root structure persist longer. The goal was therefore less about offering a prescriptive set of model parameters to improve legacy but simply test the direction and potential sensitivity of legacy to ecosystems when roots are allowed to forage. We hypothesized that dynamic roots could force an ecosystem to be poorly conditioned when the initial stressor was relieved, leading to subsequent declines in productivity and consequently an extended memory of a perturbation such as drought. Alternatively, the adjusted root profiles could prove to better condition the system for future limitation if the cause of the initial stress (e.g.

moisture stress) continued to be a persistent limiting factor. In this case, dynamic root would reduce the legacy of the initial stressor. This hypothesized role of roots assumes roots enter a perturbation in an optimal state however we note that due to life history, long lived species may have root profiles that are pre-conditioned for extreme stress events. This would further determine the sensitivity of roots profiles to stress. Our results have shown that depending on the background water stress of a site, both enhanced and reduced legacy emerge as a result of root foraging (Figs. 5 and 9).

One of the first challenges to understanding the role of roots in driving legacy, was the question of how roots in fact respond to perturbation. Overwhelmingly, ecosystems across all climatic and PFT groups, irrespective of the initialized root profile, showed a deepening of roots following negative GPP events (Fig. 6). This confirms that within the simulations, water stress was the dominant driver of GPP events and that foraging for water systematically leads to deeper root profiles (Grossiord et al. 2017; Drewniak 2019; Canadell et al. 1996; Doughty et al. 2014). The changes in root distribution were generally modest which reflects that foraging deeper comes at hydraulic costs and the expense of nutrient access and so a radical redistribution of roots would be highly detrimental (Dybzinski et al. 2011) (Fig. 7). The changes in root distribution tended to shift around an inflection at 10 cm (loss of roots above this depth) and the altered profile tended to fade away within 8-10 months (Fig. 6). Both the direction and magnitude of the changes in root profile from the simulations are broadly consistent with site level observations (Joslin et al. 2000; Schenk and Jackson 2002). However, because the model imposes limits on maximum rooting depth, the simulations miss the complex role that rarified deep roots play in providing a buffer from water stress while allowing for shallow roots to continue to access nutrients and take advantage of small rainstorms (Germon et al. 2020). Nonetheless, the effect on legacy that comes from ecosystems deepening their roots in response to negative stressors, can be explained through a set of simple conceptual models that we describe below.

In semi-arid ecosystems that are typically water stressed, the deeper root profile after negative stress events remains favorable and allows these systems - whether they are forests, shrubs or grasslands - to recover more quickly. However, in these same systems the shallowing of the root system following positive events tends to leave the vegetation vulnerable to subsequent water

stress - which is the norm for systems with aridity index of less than 1 - and thus the systems cannot maintain positive GPP anomalies following the initial event (Fig. 9). In other words, dynamic roots diminish the legacy of both positive and negative events in semi-arid systems. A similar effect emerged in the forest irrigation experiment described by Zweifel et al. (2020), where following multiple years of irrigating, a semi-arid forest invested more heavily in root systems. When the irrigation experiment ended, the forest under-performed the control during dry periods of the year. In other words, this artificially-imposed pluvial event led the system to be poorly conditioned for the more normally water stressed state of the ecosystem.

The behavior in semi-arid ecosystems was inverted in wetter systems where the deeper root profile following negative events led to sustained negative productivity anomalies because the deeper root profile reduced access to nutrients while the increased access to water was not favorable. These systems also shallowed their roots during positive GPP events, which sustained the positive productivity anomalies because of the increased access to nutrients at minimal expense to the lost access to deeper water pools. Therefore, the wetter systems showed an increased legacy in response to root foraging (Fig. 9). The more surprising result was observed in the hyper-arid sites which, unlike the semi-arid sites, showed enhanced legacy. We hypothesize that this dynamic arose because the deeper root profiles following negative GPP events, led to reduced access to surface soil moisture pools from small precipitation events and therefore extended legacy from stress events. Similarly, the shallower roots after positive events enhanced access to these surface water pools and thus extended the positive GPP anomaly. The ability to take advantage of these small rain events is critical to the water demands in these ecosystems (Ritter et al. 2020) and so whereas the deeper root system will expedite recovery in semi-arid systems, the driest systems are penalized by lost access to near surface soil water (Sala et al. 2012). The actual dynamics in these ecosystems are likely to be strongly affected by the development of dimorphic root profiles with some extremely deep roots (Dawson and Pate 1996). The inability of the model to reproduce very deep roots means that the modeled effect of roots on legacy in these very dry systems is somewhat artificial. Despite the more counter-intuitive results in the hyper-arid systems, the broad pattern of deepening roots from negative events and shallowing roots from positive events leads to effects on legacy that can be readily predicted based on whether a system is generally water stressed or not

(Sala et al. 2012).

Although most of the ecosystems in these simulations behaved as water-stressed and thus foraged for deep water, a smaller subset of grid cells had strongly competing water and nutrient limitations which resulted in the dimorphic root response captured by Cluster 3 (Figs. 7 and 9). These grid cells displayed a response to stress showing loss of surface roots ($\leq$2 cm) and deep roots ($\geq$80 cm) while roots accumulated in the more intermediate depths. This pattern emerged as a consequence of a trade-off between optimizing water access by allocating fine roots between 10-80 cm at the expense of deeper roots that can supply only limited nutrients. This pattern only emerged in sites where the aridity index was less than 1 but, interestingly, lead to an increase in legacy in 90% of the grid cells that displayed this root allocation behavior. This dynamic is notable because it is opposite to the more common reduction in legacy at semi-arid sites discussed above. We hypothesize that following negative GPP events, the loss of both the shallow and deep root pools, sustains the negative GPP anomalies by extending both water and nutrient limitations. On the other hand, the added shallow and deeper roots after positive GPP events, can sustain the positive anomalies by meeting the demands of both the persistent water and nutrient limitations. This dimorphic pattern does not emerge in sites where the driver of stress is singularly focused on water. We highlight this case because it shows how the competing nutrient and water foraging led to a more complex pattern and one that exclusively enhances legacy, which, as noted, is a chronic issue in ESMs.

The results indicate that the effect of dynamic roots on GPP legacy can be largely explained through a consideration of background water stress and whether that co-exists with nutrient limitations. We also show that these changes in GPP legacy are equivalently mirrored by changes in transpiration legacy. The response of transpiration legacy relative to GPP was largely unaffected by the structure of the root response to stress such that, for example, the common pattern where semi-arid systems deepen their roots and expedite GPP recovery holds true for transpiration as well. One implication of this is that the more rapid recovery of transpiration as a result of dynamic roots means that the canopy will experience less sustained reductions in latent heat (or increases in sensible heat) (Yunusa et al. 2015). The presence of dynamic roots in semi-arid systems thus

reduces the effect of vegetation in sustaining surface-boundary layer feedbacks associated with drought. In addition, the more rapid recovery of transpiration would also mean that vegetation water demands would recover at the expense of, for example, enhanced runoff following a negative GPP event. This latter point goes beyond the direct topic of this study but is interesting to consider the effect that dynamic roots have on recovery from the catchment perspective. The strong coupling between GPP and transpiration is, for the most part, expected though we also note that the two fluxes can become more loosely coupled during periods of limited water stress where radiation or nutrients might limit GPP but transpiration can remain high (Berkelhammer et al. 2020). Indeed, we note one key deviation between the response of GPP and transpiration legacy to dynamic roots emerged in the tropical broadleaf evergreen systems that showed a much wider range in the response of transpiration legacy to dynamic roots relative to GPP. These are sites that were already characterized by relatively high levels of GPP legacy (Fig. 1) and this effect is thus amplified in terms of how transpiration anomalies persist. Evaporative demand is particularly high year round at these sites and slight modifications of root profiles to optimize water access, has an amplified and sustained effect on water use. While this behavior is unique to this PFT, we note that this ecosystem is widespread and transpiration from this region is critical not only to supporting regional rainfall patterns (Wright et al. 2017) but also to global humidity budgets (Worden et al. 2007). Consequently, extending the transpiration anomalies following a drought or pluvial event in the tropical evergreen forests have impacts that may be widespread. However, simulations with a coupled land and atmosphere would be needed to quantify this effect.

5. Conclusion

The addition of dynamic roots into an Earth System Model has clear impacts on legacy effects in both GPP and transpiration. While previous studies have suggested models tended to lack ecosystem dynamics needed to capture endogenous legacy, the addition of roots and this added complexity does not universally increase legacy in carbon and water fluxes. In fact, across many regions, particularly semi arid zones, the effect is the opposite. In these ecosystems that are chronically water stressed, the addition of dynamic roots acts to enhance coupling of ecosystem water and carbon fluxes to exogenous forcing. This result shows that while the structural

components of the ecosystem - i.e. the root distribution - exhibited persistence after the event, there was no outward manifestation of this in terms of changes on total carbon uptake or water use. This is complementary to the site level study of Kannenberg et al. (2020), who noted that the GPP quickly rebounded from a drought while canopy structure remained perturbed. In the end, the addition of dynamic roots neither degraded nor enhanced the performance of the model with respect to capturing realistic legacy but the results highlight the critical role that belowground carbon dynamics can have in recovery from perturbation (Phillips et al. 2016). This is a critical observation in light of the potential compounding effects that increasingly frequent stress events will have on ecosystem function (Szejner et al. 2020). Future work would benefit from the inclusion of more holistic root dynamic including dynamic morphology, adding more complexity to the turnover time of root carbon pools (Matamala et al. 2003), dynamic allocation schemes between aboveground and belowground pools Lu et al. (2019) as well as the addition of deeper roots pools (Fan et al. 2017) and hydraulic redistribution. As the representation of root processes becomes more complex in ESMs, testing the effects of these dynamics on ecosystem legacy will serve as a useful tool to develop hypotheses about belowground sources of ecosystem legacy that in turn influence aboveground land surface-atmosphere coupling.

Acknowledgments. The authors would like to acknowledge DOE grant DE-SC0020285 to MB, MGM and BD for supporting this work.

Data availability statement. All simulations utilized in this manuscript have been archived and made publicly through the ESS-DIVE data repository: `https://ess-dive.lbl.gov/`. The aridity index data was utilized as previously published and downloaded from: `https://cgiarcsi.community/data/global-aridity-and-pet-database/`. The satellite GPP data (i.e. FLUXSAT) was downloaded from: `https://avdc.gsfc.nasa.gov/pub/tmp/FluxSat_GPP/`

TABLE 1. Names of PFTs and their associated numeric and acronym labels

PFT	*Numeric*	*Acronym*
Needleaf Evergreen Temperature Tree	2	NETT
Needleaf Evergreen Boreal Tree	3	NEBT
Needleaf Deciduous Boreal Tree	4	NDBT
Broadleaf Evergreen Tropical Tree	5	BETrT
Broadleaf Evergreen Temperate Tree	6	BETT
Broadleaf Deciduous Tropical Tree	7	BDTrT
Broadleaf Deciduous Temperate Tree	8	BDTT
Broadleaf Deciduous Boreal Tree	9	BDBT
Broadleaf Evergreen Shrub	10	BES
Broadleaf Deciduous Temperate Shrub	11	BDTS
Broadleaf Deciduous Boreal Shrub	12	BDBS
C3 Arctic Grass	13	C3A
C3 Non-Arctic Grass	14	C3G
C4 Grass	15	C4
C3 Crop	16	C3C
C3 Irrigated	17	C3I
Corn	18	CO
Irrigated Corn	19	CI
Spring Temperate Cereal	20	STC
Spring Temperate Cereal Irrigated	21	STCI
Winter Temperate Cereal	22	WTC
Irrigated Winter Temperate Cereal	23	WTCI
Soybean	24	SO
Irrigated Soybean	25	SOI

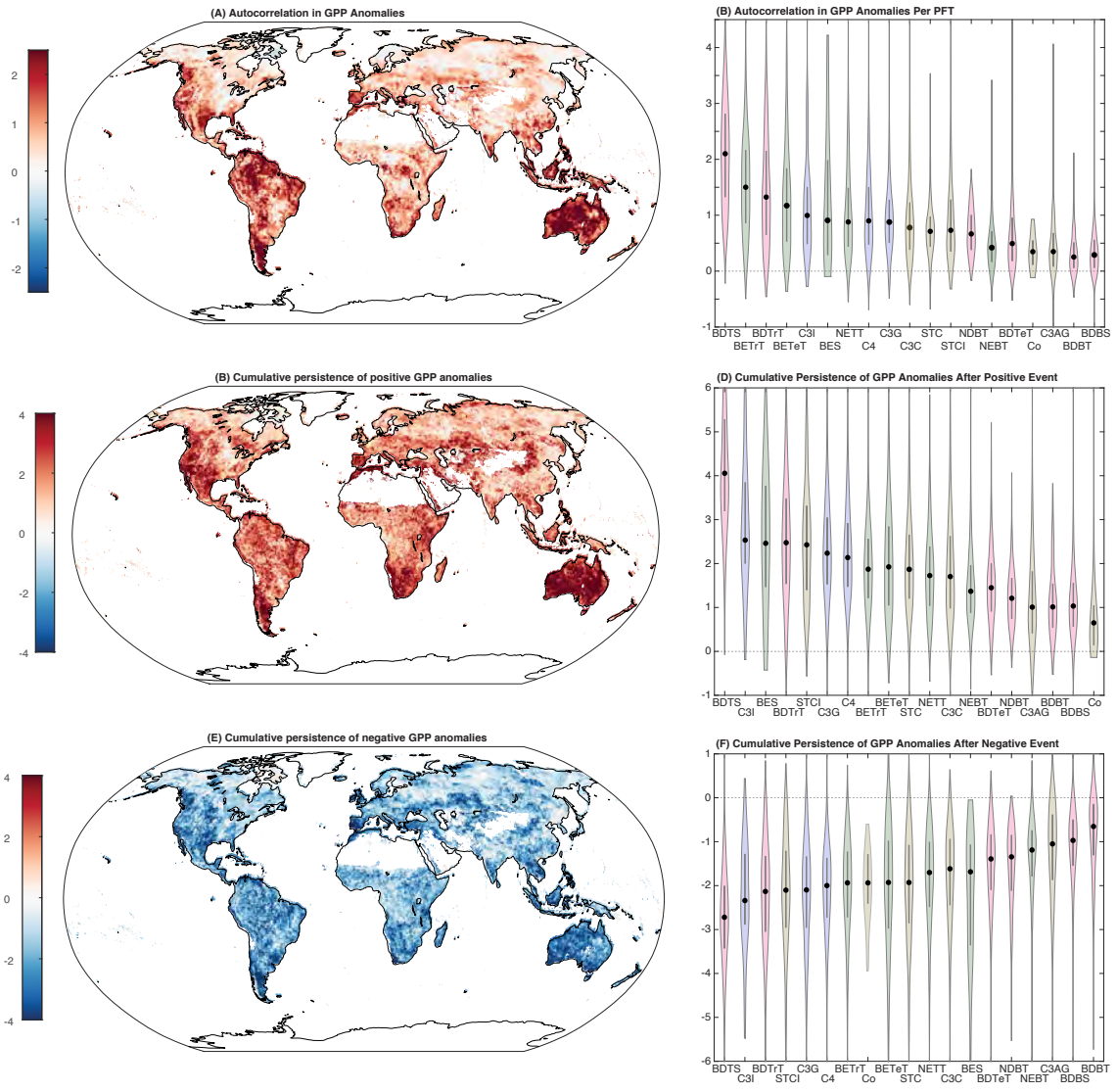

FIG. 1. Average legacy strength derived from the FluxSat global GPP product (Joiner et al. 2018). (A and B) Legacy derived from the autocorrelation of GPP anomalies in both map view and binned by PFTs, (B and C) Legacy derived as the sum of GPP anomalies following positive GPP events in both map view and binned by PFTs and (D and E) Legacy derived as the sum of GPP anomalies following negative GPP events in both map view and binned by PFTs (Table 1).

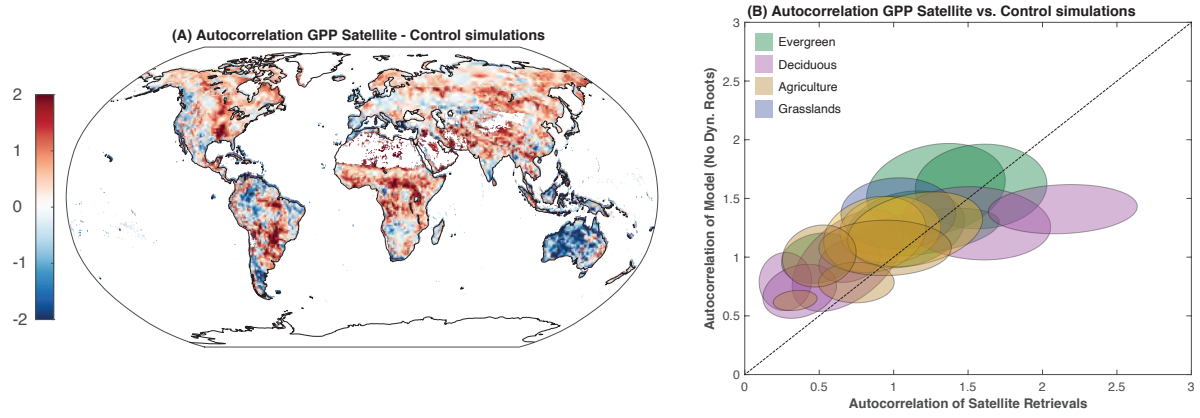

667 FIG. 2. (A) Difference in the strength of legacy (as derived using autocorrelation method) between the satellite
668 data (Figure 1A) and control E3SM simulations with no dynamic roots. (B) The relationship between the satellite
669 legacy and control simulations binned by PFT and plotted as a violin plot.

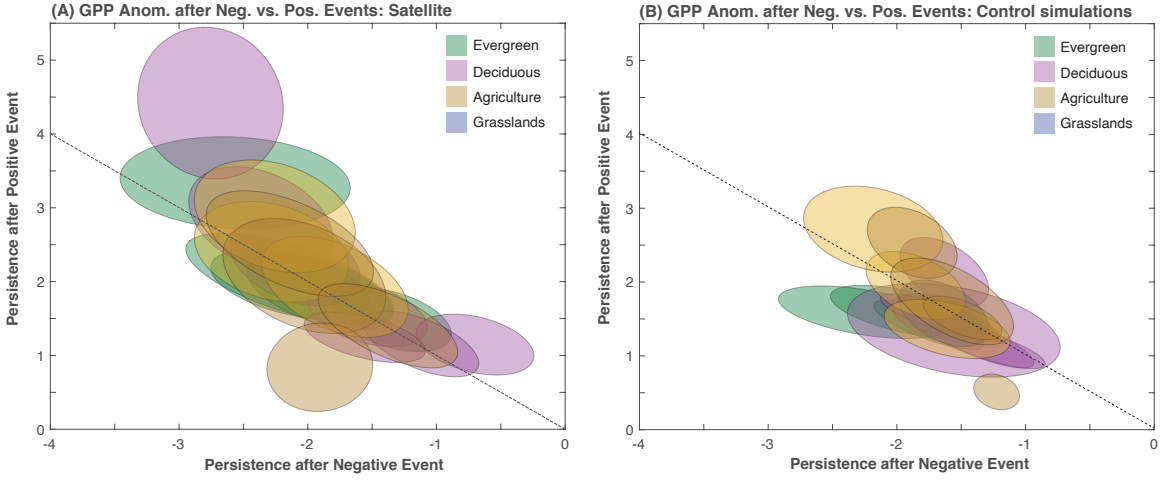

670 FIG. 3. Relationship between scale of legacy response to positive and negative GPP events based on (A)
671 Satellite data and (B) control simulations without dynamic roots. The global data was broken up into each of the
672 PFTs in Table 1 and the range of data from each PFT is indicated by the bubbles which are color coded based on
673 broader PFT classifications as indicated in the figure.

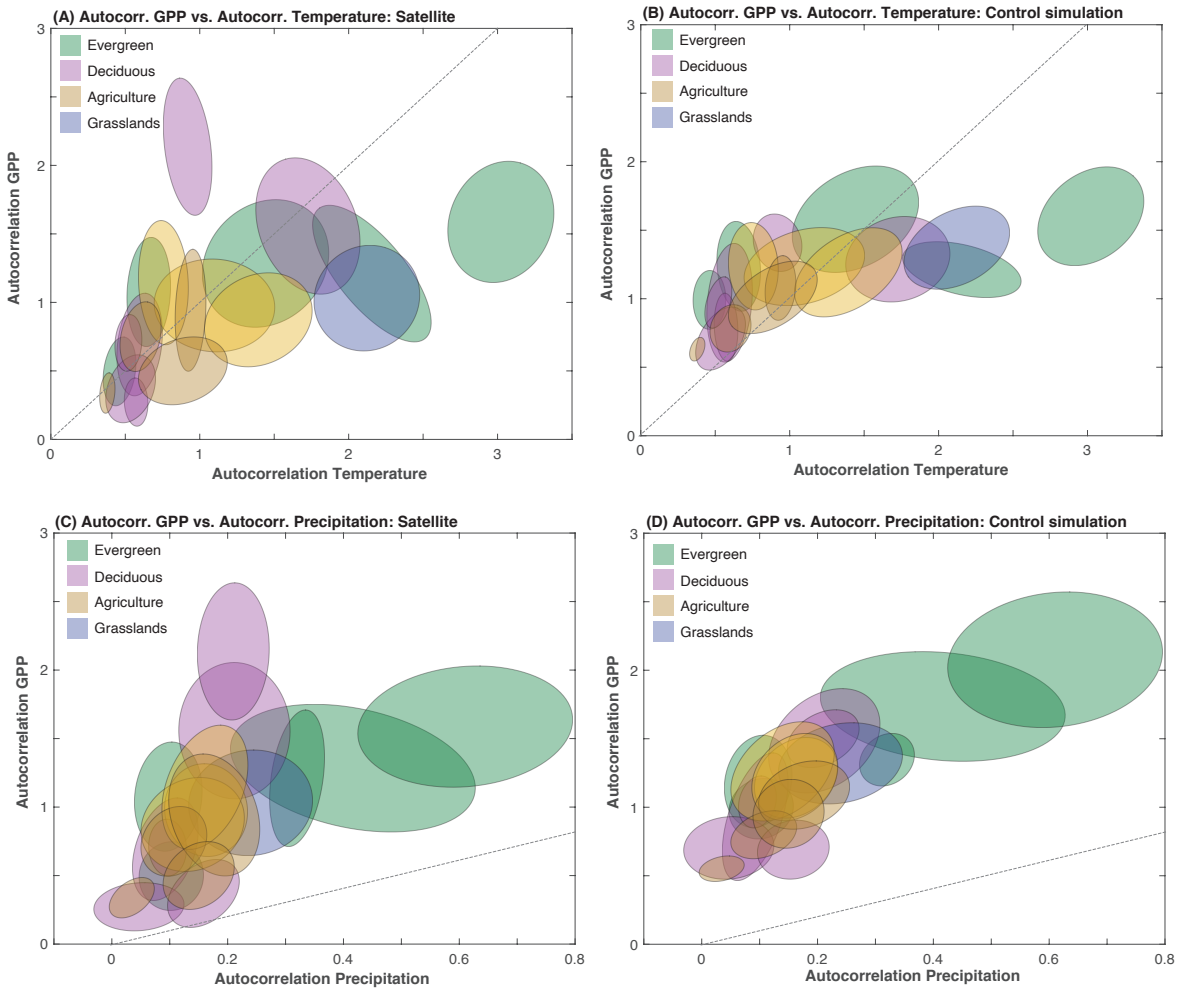

674 FIG. 4. Relationship between legacy strength of GPP vs. legacy strength of temperature (A and B) and
675 precipitation (C and D). The lines indicate a 1:1 relationship where the legacy of GPP is fully explained by the
676 legacy of the climate forcing. The first column (A and C) shows results from the satellite data and the second
677 column (B and D) shows the results from the control simulations with no dynamic roots. As with the previous
678 figure, the global data was broken up into each of the PFTs in Table 1 and the range of data from each PFT is
679 indicated by the bubbles which are color coded based on broader classifications as indicated in the figure.

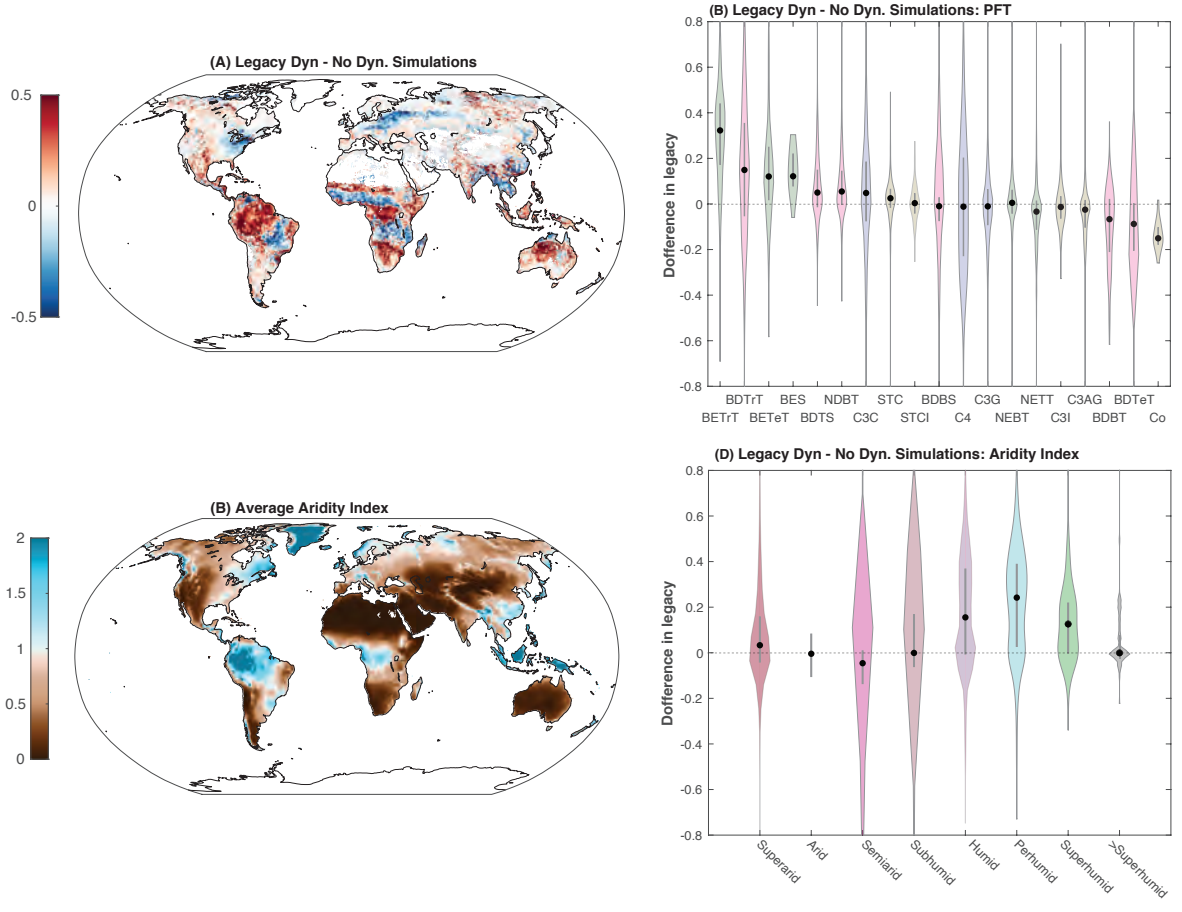

680 FIG. 5. (A and B) Difference in legacy between simulations with and without dynamic roots in both map view
681 and broken up by PFT. (D) The data from Panel A was binned according to average aridity index for each grid
682 cell. (C) Global averaged aridity index values are shown here for reference (Trabucco and Zomer 2018).

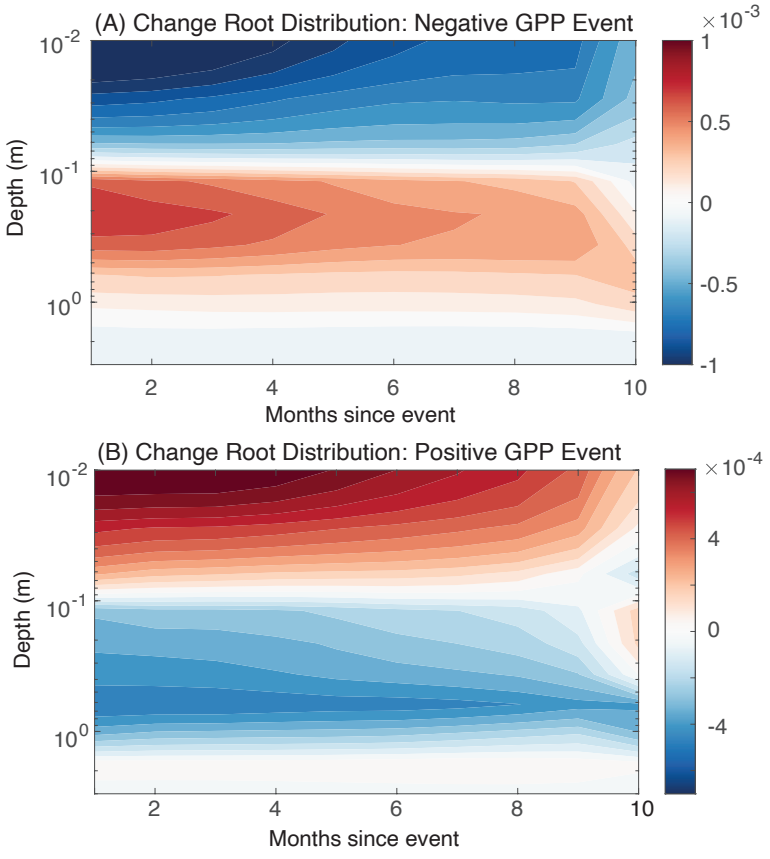

683 FIG. 6. The average change in root distribution as a function of depth in the 10 months following a negative
684 (A) and positive GPP (B) event. The red tones are associated with depths where fine roots has increased relative
685 to the mean root profile at the grid cell and blue tones indicate depths where fine roots are in deficit relative to
686 average.

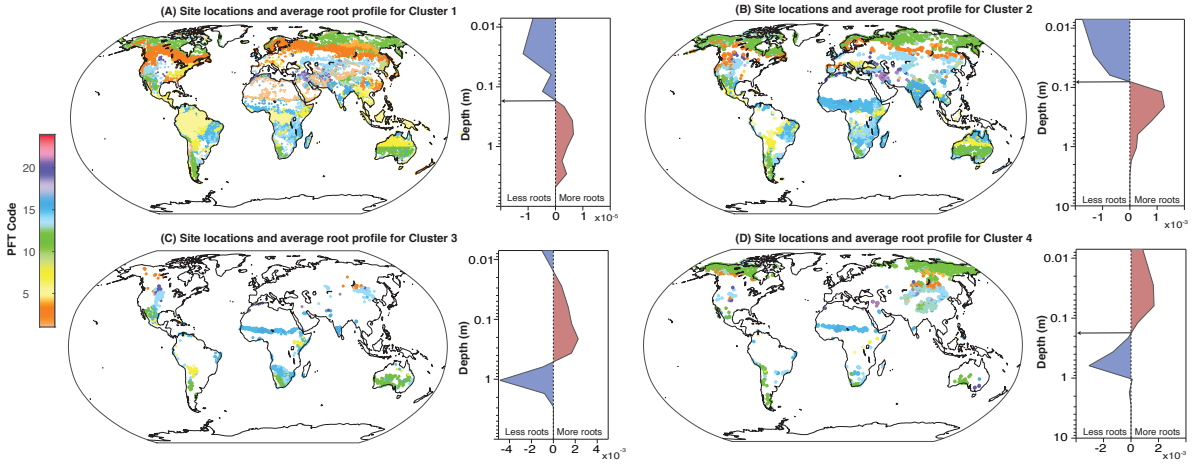

687 FIG. 7. Results from the clustering analysis showing the locations/PFTs and profiles of the root fraction
688 anomalies following **negative** GPP events for 4 of the clusters. Clusters 1 (A) and 2 (B) are the dominant
689 structure where fine roots accumulate in the lower depths at the expense of the surface soils. Clusters 3 (C) and
690 4 (D) provide examples of the less common situation where fine roots accumulate nearer the surface following
691 negative GPP events. The arrows in A, B and D are used as a reference to highlight the transition depth associated
692 with either the loss or gain of fine roots. This is not labeled in C because there is a dimorphic change associated
693 with this cluster.

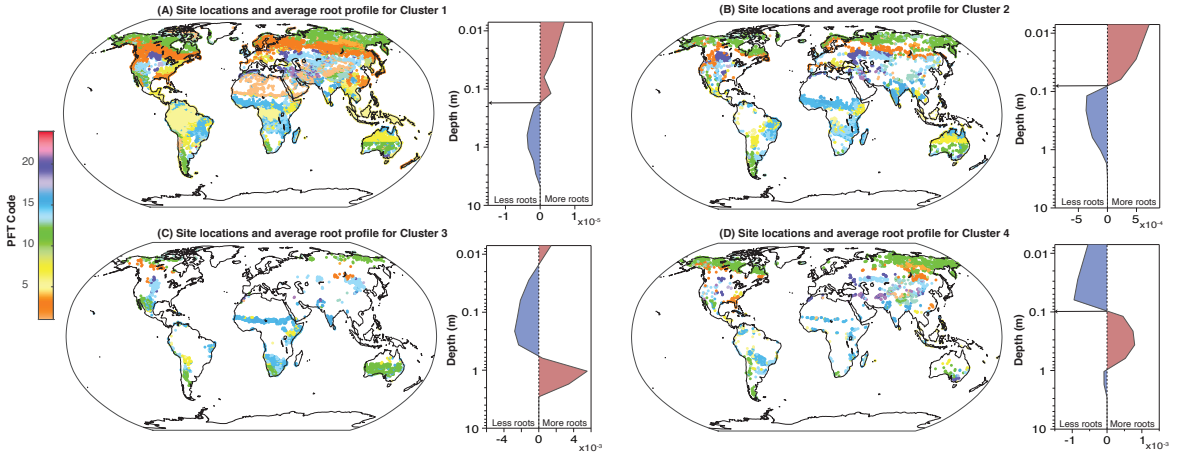

694 FIG. 8. Results from the clustering analysis showing the locations/PFTs and structure of the changes in root
695 profiles following **positive** GPP events for 4 of the clusters. Clusters 1 (A) and 2 (B) are the dominant structure
696 where fine roots accumulate near the surface at the expense of the deeper horizons. Clusters 3 (C) and 4 (D)
697 provide examples of the less common situation where fine roots accumulate at depth following positive GPP
698 events. The arrows in A, B and D are used as a reference to highlight the transition depth associated with either
699 the loss or gain of fine roots. This is not labeled in C because there is a dimorphic change associated with this
700 cluster.

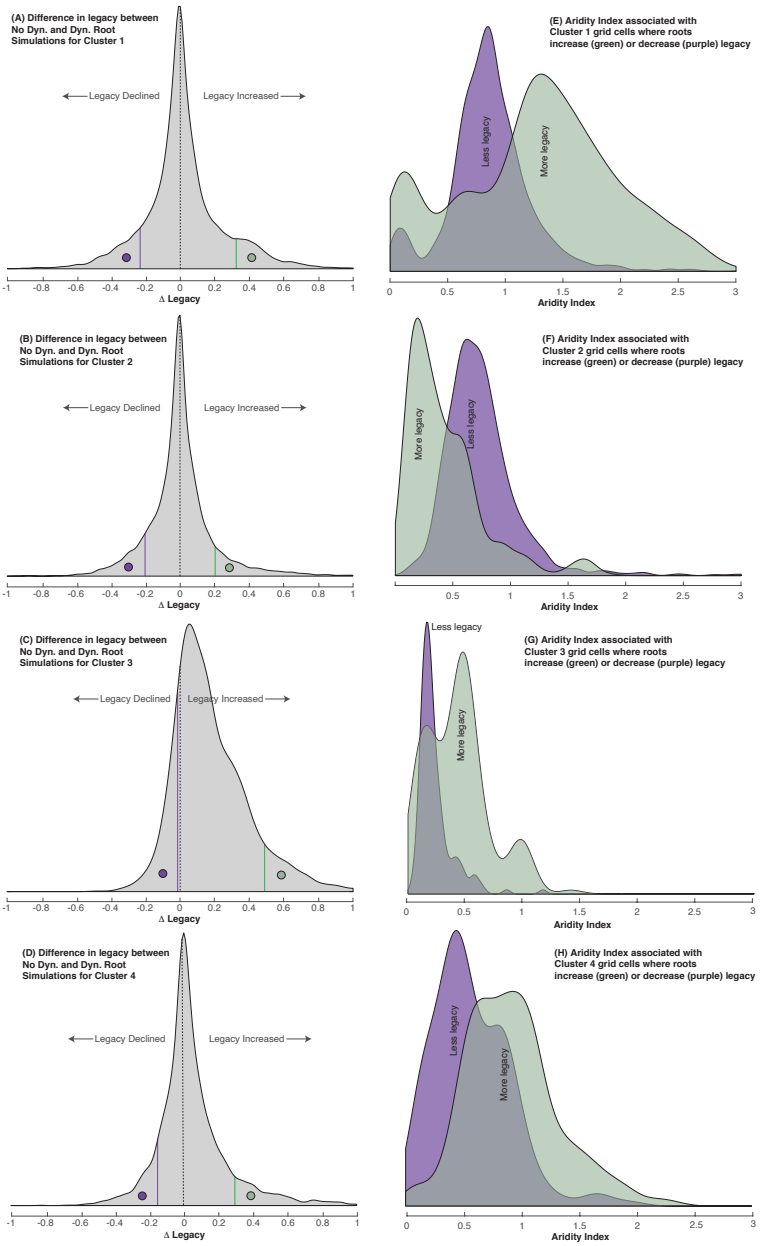

FIG. 9. The left column (A-D) shows the distribution of the change in ecosystem legacy (i.e. Δ *Legacy*) for all the points associated with Cluster 1 (A), Cluster 2 (B), Cluster 3 (C) and Cluster 4 (D) as shown in the maps in Figures 7 and 8. Values of 0 (the dotted line) mean that the change in root profile associated with the GPP event had no effect on the ecosystem legacy strength. The colored lines indicate the 10^{th} and 90^{th} percentiles which were used as the threshold to capture the grid cells where the addition of root foraging drove a large increase (green) or decrease (purple) in legacy. The right column (E-H) shows the distribution in the aridity index associated with the grid cells that had large increases (green) or large decreases (purple) in legacy. For example, the two distributions in Panel F indicate that the particular root response associated with Cluster 2 increased legacy at wet sites (i.e. aridity index $\geq$1) and decreased legacy at semi-arid (i.e. aridity index $\sim$ 0.5) sites.

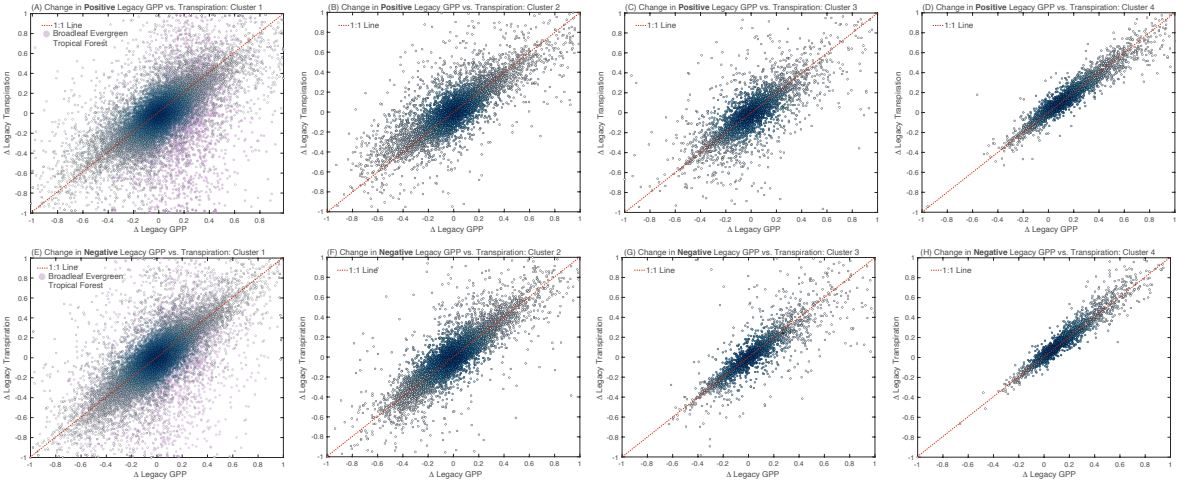

FIG. 10. The relationship between the change in ecosystem legacy (i.e. Δ *Legacy*) associated with dynamic roots for GPP (x-axis) and transpiration (y-axis). The top row (A-D) shows the GPP vs. transpiration legacy effects for each of the 4 clusters discussed in Figures 7-9 associated with positive GPP events. The bottom row shows (E-H) shows the changes in GPP vs. transpiration legacy for each of the 4 clusters discussed in Figures 7-9 associated with negative GPP events. In panels A and E, the points associated with Broadleaf Evergreen Tropical Forests were separated because data from these grid cells had a clearly distinct response. The red line in all plots show the 1:1 line for reference. The coloring of the data is used to indicate relative density of points.

References

Amenu, G. G., P. Kumar, and X.-Z. Liang, 2005: Interannual variability of deep-layer hydrologic memory and mechanisms of its influence on surface energy fluxes. *Journal of climate*, **18 (23)**, 5024–5045.

Anderegg, L. D., W. R. Anderegg, J. Abatzoglou, A. M. Hausladen, and J. A. Berry, 2013: Drought characteristics' role in widespread aspen forest mortality across colorado, usa. *Global Change Biology*, **19 (5)**, 1526–1537.

Anderegg, W. R., and Coauthors, 2015: Pervasive drought legacies in forest ecosystems and their implications for carbon cycle models. *Science*, **349 (6247)**, 528–532.

Arora, V. K., 2002: The use of the aridity index to assess climate change effect on annual runoff. *Journal of hydrology*, **265 (1-4)**, 164–177.

Belk, E. L., D. Markewitz, T. C. Rasmussen, E. J. M. Carvalho, D. C. Nepstad, and E. A. Davidson, 2007: Modeling the effects of throughfall reduction on soil water content in a brazilian oxisol under a moist tropical forest. *Water Resources Research*, **43 (8)**.

Berkelhammer, M., C. Still, F. Ritter, M. Winnick, L. Anderson, R. Carroll, M. Carbone, and K. Williams, 2020: Persistence and plasticity in conifer water-use strategies. *Journal of Geophysical Research: Biogeosciences*, **125 (2)**, e2018JG004 845.

Bloom, A. J., F. S. Chapin III, and H. A. Mooney, 1985: Resource limitation in plants-an economic analogy. *Annual review of Ecology and Systematics*, **16 (1)**, 363–392.

Bouda, M., and J. E. Saiers, 2017: Dynamic effects of root system architecture improve root water uptake in 1-d process-based soil-root hydrodynamics. *Advances in Water Resources*, **110**, 319–334.

Brunner, I., E. G. Pannatier, B. Frey, A. Rigling, W. Landolt, S. Zimmermann, and M. Dobbertin, 2009: Morphological and physiological responses of scots pine fine roots to water supply in a dry climatic region in switzerland. *Tree Physiology*, **29 (4)**, 541–550.

Bunde, A., U. Büntgen, J. Ludescher, J. Luterbacher, and H. Von Storch, 2013: Is there memory in precipitation? *Nature climate change*, **3 (3)**, 174–175.

753 Campioli, M., and Coauthors, 2016: Evaluating the convergence between eddy-covariance and
754 biometric methods for assessing carbon budgets of forests. *Nature communications*, **7 (1)**, 1–12.

755 Canadell, J., R. Jackson, J. Ehleringer, H. Mooney, O. Sala, and E.-D. Schulze, 1996: Maximum
756 rooting depth of vegetation types at the global scale. *Oecologia*, **108 (4)**, 583–595.

757 Dawson, T. E., and J. S. Pate, 1996: Seasonal water uptake and movement in root systems of
758 Australian phraeatophytic plants of dimorphic root morphology: a stable isotope investigation.
759 *Oecologia*, **107 (1)**, 13–20.

760 Dewar, R. C., A. R. Ludlow, and P. M. Dougherty, 1994: Environmental influences on carbon
761 allocation in pines. *Ecological Bulletins*, 92–101.

762 Dirmeyer, P., X. Gao, and T. Oki, 2002: The second global soil wetness project (gswp2). *Interna-*
763 *tional GEWEX Project Office Publication*, **37**, 75.

764 Donat, M. G., A. J. Pitman, and O. Angélil, 2018: Understanding and reducing future uncertainty
765 in midlatitude daily heat extremes via land surface feedback constraints. *Geophysical Research*
766 *Letters*, **45 (19)**, 10–627.

767 Doughty, C. E., and Coauthors, 2014: Allocation trade-offs dominate the response of tropical
768 forest growth to seasonal and interannual drought. *Ecology*, **95 (8)**, 2192–2201.

769 Drewniak, B., 2019: Simulating dynamic roots in the energy exascale earth system land model.
770 *Journal of Advances in Modeling Earth Systems*, **11 (1)**, 338–359.

771 Dybzinski, R., C. Farrior, A. Wolf, P. B. Reich, and S. W. Pacala, 2011: Evolutionarily stable
772 strategy carbon allocation to foliage, wood, and fine roots in trees competing for light and
773 nitrogen: an analytically tractable, individual-based model and quantitative comparisons to
774 data. *The American Naturalist*, **177 (2)**, 153–166.

775 El Masri, B., S. Shu, and A. K. Jain, 2015: Implementation of a dynamic rooting depth and
776 phenology into a land surface model: Evaluation of carbon, water, and energy fluxes in the high
777 latitude ecosystems. *Agricultural and Forest Meteorology*, **211**, 85–99.

778 Fan, Y., G. Miguez-Macho, E. G. Jobbágy, R. B. Jackson, and C. Otero-Casal, 2017: Hydrologic
779 regulation of plant rooting depth. *Proceedings of the National Academy of Sciences*, 201712381.

Fischer, E. M., S. I. Seneviratne, D. Lüthi, and C. Schär, 2007: Contribution of land-atmosphere coupling to recent european summer heat waves. *Geophysical Research Letters*, **34 (6)**.

Flower, C. E., and M. A. Gonzalez-Meler, 2015: Responses of temperate forest productivity to insect and pathogen disturbances. *Annual review of plant biology*, **66**, 547–569.

Galiano, L., J. Martínez-Vilalta, and F. Lloret, 2011: Carbon reserves and canopy defoliation determine the recovery of scots pine 4 yr after a drought episode. *New Phytologist*, **190 (3)**, 750–759.

Gazol, A., and Coauthors, 2020: Drought legacies are short, prevail in dry conifer forests and depend on growth variability. *Journal of Ecology*, **108 (6)**, 2473–2484.

Germon, A., J.-P. Laclau, A. Robin, and C. Jourdan, 2020: Tamm review: Deep fine roots in forest ecosystems: Why dig deeper? *Forest Ecology and Management*, **466**, 118 135.

Golaz, J.-C., and Coauthors, 2019: The doe e3sm coupled model version 1: Overview and evaluation at standard resolution. *Journal of Advances in Modeling Earth Systems*, **11 (7)**, 2089–2129.

Gonzalez-Valencia, R., F. Magana-Rodriguez, O. Gerardo-Nieto, A. Sepulveda-Jauregui, K. Martinez-Cruz, K. Walter Anthony, D. Baer, and F. Thalasso, 2014: In situ measurement of dissolved methane and carbon dioxide in freshwater ecosystems by off-axis integrated cavity output spectroscopy. *Environmental science & technology*, **48 (19)**, 11 421–11 428.

Grossiord, C., and Coauthors, 2017: Warming combined with more extreme precipitation regimes modifies the water sources used by trees. *New Phytologist*, **213 (2)**, 584–596.

Hendrick, R. L., and K. S. Pregitzer, 1996: Temporal and depth-related patterns of fine root dynamics in northern hardwood forests. *Journal of Ecology*, 167–176.

Herzog, C., J. Steffen, E. G. Pannatier, I. Hajdas, and I. Brunner, 2014: Nine years of irrigation cause vegetation and fine root shifts in a water-limited pine forest. *PloS one*, **9 (5)**, e96 321.

Jiang, P., H. Liu, S. Piao, P. Ciais, X. Wu, Y. Yin, and H. Wang, 2019: Enhanced growth after extreme wetness compensates for post-drought carbon loss in dry forests. *Nature communications*, **10 (1)**, 1–9.

807 Joiner, J., Y. Yoshida, Y. Zhang, G. Duveiller, M. Jung, A. Lyapustin, Y. Wang, and C. J. Tucker,
808 2018: Estimation of terrestrial global gross primary production (gpp) with satellite data-driven
809 models and eddy covariance flux data. *Remote Sensing*, **10 (9)**, 1346.

810 Joslin, J., M. Wolfe, and P. Hanson, 2000: Effects of altered water regimes on forest root systems.
811 *The New phytologist*, **147 (1)**, 117–129.

812 Kannenberg, S. A., K. A. Novick, M. R. Alexander, J. T. Maxwell, D. J. Moore, R. P. Phillips, and
813 W. R. Anderegg, 2019: Linking drought legacy effects across scales: From leaves to tree rings
814 to ecosystems. *Global Change Biology*, **25 (9)**, 2978–2992.

815 Kannenberg, S. A., C. R. Schwalm, and W. R. Anderegg, 2020: Ghosts of the past: how drought
816 legacy effects shape forest functioning and carbon cycling. *Ecology letters*, **23 (5)**, 891–901.

817 Kaufman, L., and P. J. Rousseeuw, 2009: *Finding groups in data: an introduction to cluster*
818 *analysis*, Vol. 344. John Wiley & Sons.

819 Kolus, H. R., and Coauthors, 2019: Land carbon models underestimate the severity and duration
820 of drought's impact on plant productivity. *Scientific reports*, **9 (1)**, 1–10.

821 Kou, L., L. Jiang, X. Fu, X. Dai, H. Wang, and S. Li, 2018: Nitrogen deposition increases
822 root production and turnover but slows root decomposition in pinus elliottii plantations. *New*
823 *Phytologist*, **218 (4)**, 1450–1461.

824 Kumar, S., M. Newman, Y. Wang, and B. Livneh, 2019: Potential reemergence of seasonal soil
825 moisture anomalies in north america. *Journal of Climate*, **32 (10)**, 2707–2734.

826 Liu, Y., C. R. Schwalm, K. E. Samuels-Crow, and K. Ogle, 2019: Ecological memory of daily
827 carbon exchange across the globe and its importance in drylands. *Ecology letters*, **22 (11)**,
828 1806–1816.

829 Lu, H., W. Yuan, and X. Chen, 2019: A processes-based dynamic root growth model integrated
830 into the ecosystem model. *Journal of Advances in Modeling Earth Systems*, **11 (12)**, 4614–4628.

831 Markesteijn, L., and L. Poorter, 2009: Seedling root morphology and biomass allocation of 62
832 tropical tree species in relation to drought-and shade-tolerance. *Journal of Ecology*, **97 (2)**,
833 311–325.

Markewitz, D., S. Devine, E. A. Davidson, P. Brando, and D. C. Nepstad, 2010: Soil moisture depletion under simulated drought in the amazon: impacts on deep root uptake. *New Phytologist*, **187 (3)**, 592–607.

Matamala, R., M. A. Gonzalez-Meler, J. D. Jastrow, R. J. Norby, and W. H. Schlesinger, 2003: Impacts of fine root turnover on forest npp and soil c sequestration potential. *Science*, **302 (5649)**, 1385–1387.

McCarthy, M., and B. Enquist, 2007: Consistency between an allometric approach and optimal partitioning theory in global patterns of plant biomass allocation. *Functional Ecology*, **21 (4)**, 713–720.

McCormack, M. L., and Coauthors, 2015: Redefining fine roots improves understanding of below-ground contributions to terrestrial biosphere processes. *New Phytologist*, **207 (3)**, 505–518.

McDowell, N. G., and Coauthors, 2013: Evaluating theories of drought-induced vegetation mortality using a multimodel–experiment framework. *New Phytologist*, **200 (2)**, 304–321.

McNickle, G. G., M. A. Gonzalez-Meler, D. J. Lynch, J. L. Baltzer, and J. S. Brown, 2016: The world's biomes and primary production as a triple tragedy of the commons foraging game played among plants. *Proceedings of the Royal Society B: Biological Sciences*, **283 (1842)**, 20161 993.

Metcalfe, D. B., and Coauthors, 2008: The effects of water availability on root growth and morphology in an amazon rainforest. *Plant and Soil*, **311 (1)**, 189–199.

Miralles, D. G., P. Gentine, S. I. Seneviratne, and A. J. Teuling, 2019: Land–atmospheric feedbacks during droughts and heatwaves: state of the science and current challenges. *Annals of the New York Academy of Sciences*, **1436 (1)**, 19.

Monger, C., O. E. Sala, M. C. Duniway, H. Goldfus, I. A. Meir, R. M. Poch, H. L. Throop, and E. R. Vivoni, 2015: Legacy effects in linked ecological–soil–geomorphic systems of drylands. *Frontiers in Ecology and the Environment*, **13 (1)**, 13–19.

Ogle, K., J. J. Barber, G. A. Barron-Gafford, L. P. Bentley, J. M. Young, T. E. Huxman, M. E. Loik, and D. T. Tissue, 2015: Quantifying ecological memory in plant and ecosystem processes. *Ecology letters*, **18 (3)**, 221–235.

Ovenden, T. S., M. P. Perks, T.-K. Clarke, M. Mencuccini, and A. S. Jump, 2021: Life after recovery: Increased resolution of forest resilience assessment sheds new light on post-drought compensatory growth and recovery dynamics. *Journal of Ecology*.

Peltier, D. M., and K. Ogle, 2020: Tree growth sensitivity to climate is temporally variable. *Ecology Letters*, **23 (11)**, 1561–1572.

Phillips, R. P., I. Ibáñez, L. D'Orangeville, P. J. Hanson, M. G. Ryan, and N. G. McDowell, 2016: A belowground perspective on the drought sensitivity of forests: Towards improved understanding and simulation. *Forest Ecology and Management*, **380**, 309–320.

Poorter, H., K. J. Niklas, P. B. Reich, J. Oleksyn, P. Poot, and L. Mommer, 2012: Biomass allocation to leaves, stems and roots: meta-analyses of interspecific variation and environmental control. *New Phytologist*, **193 (1)**, 30–50.

Richardson, A. D., and Coauthors, 2015: Distribution and mixing of old and new nonstructural carbon in two temperate trees. *New Phytologist*, **206 (2)**, 590–597.

Ritter, F., M. Berkelhammer, and C. Garcia-Eidell, 2020: Distinct response of gross primary productivity in five terrestrial biomes to precipitation variability. *Communications Earth & Environment*, **1 (1)**, 1–8.

Sakschewski, B., and Coauthors, 2021: Variable tree rooting strategies are key for modelling the distribution, productivity and evapotranspiration of tropical evergreen forests. *Biogeosciences*, **18 (13)**, 4091–4116.

Sala, O., W. Lauenroth, and W. Parton, 1992: Long-term soil water dynamics in the shortgrass steppe. *Ecology*, **73 (4)**, 1175–1181.

Sala, O. E., L. A. Gherardi, L. Reichmann, E. Jobbagy, and D. Peters, 2012: Legacies of precipitation fluctuations on primary production: theory and data synthesis. *Philosophical Transactions of the Royal Society B: Biological Sciences*, **367 (1606)**, 3135–3144.

Schenk, H. J., and R. B. Jackson, 2002: Rooting depths, lateral root spreads and belowground/above-ground allometries of plants in water-limited ecosystems. *Journal of Ecology*, **90 (3)**, 480–494.

888 Seddon, A. W., M. Macias-Fauria, P. R. Long, D. Benz, and K. J. Willis, 2016: Sensitivity of
889 global terrestrial ecosystems to climate variability. *Nature*, **531 (7593)**, 229–232.

890 Szejner, P., S. Belmecheri, J. R. Ehleringer, and R. K. Monson, 2020: Recent increases in drought
891 frequency cause observed multi-year drought legacies in the tree rings of semi-arid forests.
892 *Oecologia*, **192 (1)**, 241–259.

893 Thornley, J. H., 1998: Modelling shoot [ratio] root relations: the only way forward? *Annals of*
894 *Botany*, **81 (2)**, 165–171.

895 Thornton, P. E., and N. A. Rosenbloom, 2005: Ecosystem model spin-up: Estimating steady
896 state conditions in a coupled terrestrial carbon and nitrogen cycle model. *Ecological Modelling*,
897 **189 (1-2)**, 25–48.

898 Trabucco, A., and R. J. Zomer, 2018: Global aridity index and potential evapotranspiration (et0)
899 climate database v2. *CGIAR Consort Spat Inf*.

900 Trugman, A., M. Detto, M. Bartlett, D. Medvigy, W. Anderegg, C. Schwalm, B. Schaffer, and
901 S. W. Pacala, 2018: Tree carbon allocation explains forest drought-kill and recovery patterns.
902 *Ecology Letters*, **21 (10)**, 1552–1560.

903 van der Molen, M. K., and Coauthors, 2011: Drought and ecosystem carbon cycling. *Agricultural*
904 *and Forest Meteorology*, **151 (7)**, 765–773.

905 Warren, J. M., P. J. Hanson, C. M. Iversen, J. Kumar, A. P. Walker, and S. D. Wullschleger,
906 2015: Root structural and functional dynamics in terrestrial biosphere models–evaluation and
907 recommendations. *New Phytologist*, **205 (1)**, 59–78.

908 Worden, J., D. Noone, and K. Bowman, 2007: Importance of rain evaporation and continental
909 convection in the tropical water cycle. *Nature*, **445 (7127)**, 528–532.

910 Wright, J. S., R. Fu, J. R. Worden, S. Chakraborty, N. E. Clinton, C. Risi, Y. Sun, and L. Yin, 2017:
911 Rainforest-initiated wet season onset over the southern amazon. *Proceedings of the National*
912 *Academy of Sciences*, **114 (32)**, 8481–8486.

913 Yunusa, I. A., D. Eamus, D. Taylor, R. Whitley, W. Gwenzi, A. R. Palmer, and Z. Li, 2015:
914 Partitioning of turbulent flux reveals contrasting cooling potential for woody vegetation and

915 grassland during heat waves. *Quarterly Journal of the Royal Meteorological Society*, **141 (692)**,
916 2528–2537.

917 Zweifel, R., and Coauthors, 2020: Determinants of legacy effects in pine trees–implications from
918 an irrigation-stop experiment. *The New Phytologist*, **227 (4)**, 1081.